BIOSCIENCE JOURNAL

EFFECT OF MINI-SCREW POSITIONING AND QUANTITY IN A MARPE EXPANDER IN A YOUNG ADULT CLEFT PALATE PATIENT: A FINITE ELEMENT STUDY

Angela Maria Bautista PATIÑO[1], Nathalia de Oliveira DOMINGOS[1], Douglas Teixeira da SILVA[1], Ki Beom KIM[2], Carlos José SOARES[3], Guilherme de Araújo ALMEIDA[4]

[1]Postgraduate Program in Dentistry, Universidade Federal de Uberlândia, Uberlândia, Minas Gerais, Brazil.
[2]Department of Orthodontics, Saint Louis University, MO, United States.
[3]Department of Restorative Dentistry, School of Dentistry, Universidade Federal de Uberlândia, Uberlândia, Minas Gerais, Brazil.
[4]Division of Orthodontics, Universidade Federal de Uberlândia, Uberlândia, Minas Gerais, Brazil.

How to cite: PATIÑO, A.M.B., et al. Effect of mini-screw positioning and quantity in a MARPE expander in a young adult cleft palate patient: a finite element study. *Bioscience Journal*. 2026, **42**, e42010. https://doi.org/10.14393/BJ-v42n0a2026-80927

Abstract

This study aimed to evaluate the influence of mini-screw position and number in mini-screw-assisted rapid palatal expansion (MARPE) expanders in a patient with cleft lip and palate (CLP). A cone-beam computed tomography scan of a patient aged 17 years with bilateral complete CLP was used to construct six finite element models with MARPE expanders: three bone-borne and three tooth-bone-borne configurations, varying by mini-screw number (two or three) and position (anterior or posterior). Each expander was transversely activated to achieve 1.0 mm expansion. Equivalent elastic strain (με) distributions were assessed in the maxillary palatal bone, dentoalveolar bone, and anchoring teeth. Deformation patterns in the palate and alveolar ridges (<4,000 με) were influenced by both mini-screw number and, more significantly, position. The presence of at least one mini-screw was critical for generating strain in the anterior palate. Expander arms produced notable strain at the insertion sites of banded anchoring teeth (<100 με). Mini-screw position appeared more influential than quantity in determining strain distribution. An anterior mini-screw was essential for inducing anterior palatal stress, while expander arms, regardless of mini-screw configuration, contributed to stress distribution across anchoring teeth and posterior alveolar ridges.

Keywords: Bone screws. Cleft lip. Cleft palate. Finite elements analysis. Maxillary exp ansion.

Corresponding author:
Guilherme de Araújo Almeida
guilhermealmeida@ufu.br

Received: 29 December 2025
Accepted: 17 March 2026
Published: 24 April 2026

1. Introduction

Cleft lip and palate (CLP) is a common congenital deformity caused by incomplete fusion of the maxillary and palatine processes, resulting in functional and esthetic impairments of the craniofacial complex (Cobourne 2004). A frequent manifestation is lateral maxillary constriction, predominantly in the anterior region, which often necessitates maxillary expansion (Yang et al. 2012).

Various expander types are selected according to bone resistance. In cases of increased resistance, devices with enhanced dentoskeletal anchorage are required. Mini-screw-assisted rapid palatal expansion (MARPE), with variable mini-screw number and position, effectively overcomes this resistance (Lagravere et al. 2010; Mathew et al. 2016; Moon et al. 2020) and facilitates correction of maxillary atresia in late adolescents and young adults (Mathew et al. 2016; Moon et al. 2020; Lee et al. 2014). However, cleft morphology may restrict mini-screw placement and number, potentially reducing expander efficiency. Additionally, patients with cleft palate frequently present increased palatal soft tissue thickness, limiting the transmucosal portion available for bicortical anchorage in palatine bone. In such conditions, connecting expander screws to posterior teeth (tooth-bone-borne configuration) enhances stability (Holberg et al. 2007; Pan et al. 2007; Mathew et al. 2016; Lee et al. 2016).

This study aimed to evaluate the effects of MARPE bone-borne (BB) and tooth-bone-borne (TBB) expanders on palatal and dentoalveolar structures in patients with cleft lip and palate, considering variations in mini-screw number and position, using finite element analysis.

2. Material and Methods

This study was approved by the ethics committee of the National University of Colombia and Pediatric Hospital *La Misericordia* (protocol B. CIEFO-243-18). A cone-beam computed tomography scan was obtained from the image database of the Orthodontic Department of Pediatric Hospital *La Misericordia*, Bogotá, DC, Colombia.

A maxillary scan of a patient aged 17 years with bilateral complete cleft lip and palate, previously treated with a secondary cancellous iliac crest bone graft at age 9 years prior to eruption of permanent canines, was analyzed. The patient presented complete permanent dentition to the second molars, absence of the right central and lateral incisors, and transposition involving the canines and first premolars.

A structural, nonlinear three-dimensional (3D) finite element model was developed from a cone-beam computed tomography scan (CS9300 Carestream, 90 Kv, 15 mA, field of view 10 x 5 cm, 0.18 mm slice thickness, 0.3 mm voxel size) using Mimics software (version 21.0; Materialise, Leuven, Belgium). The maxilla was segmented from the incisal edges to the zygomatic arch, and tissues, including cortical bone, cancellous bone, enamel, and dentin, were differentiated using density thresholding (Jaecques et al. 2004; Pessoa et al. 2010). A 0.2 mm periodontal ligament layer was incorporated (Pessoa et al. 2010) onto tooth roots via Boolean operations (Kronfeld 1931; Jaecques et al. 2004). Following segmentation, three-dimensional surface models were exported in stereolithography (STL) format, while orthodontic bands and expander connecting arms were designed in 3-Matic software 19 (version 18.0; Materialise, Leuven, Belgium).

The STL files were imported into MSC Patran 2010 (MSC Software Corporation, Santa Ana, CA, USA) and discretized using tetrahedral elements. The resulting mesh was imported into the MSC finite element analysis software package (MSC Marc/Mentat, MSC Software) for structural analysis. The model included 134 tetrahedral element types, with shared nodes between bone and mini-screw systems to ensure interface continuity. Boundary conditions fixed nodes on the superior maxillary surface, excluding the palatal region, in x-(horizontal), y-(vertical), and z-directions, reflecting minimal or no mobility due to craniofacial articulations. Mesh convergence was achieved by refining contact interfaces, geometric discontinuities, and regions of interest (second premolars, molars, and peri-screw areas) until peak stress and displacement variations were <1%.

Material properties, including elastic modulus and Poisson ratio, were assigned from the literature (Table 1) (Sano et al. 1994; Rees and Jacobsen 1997; Carter and Hayes 1997; Zarone et al. 2006; Lee et al. 2014; Matsuyama et al. 2015). Bonded interfaces were defined to prevent relative displacement between

structures, ensuring structural continuity and eliminating maxillary rotation. Components of the expander screw requiring interaction were considered rigid.

Table 1. Material properties of the evaluated structures.

Structure	Elastic modulus (MPa)	Poisson's ratio
Enamel	84.100	0.30
Dentin	18.600	0.31
Periodontal ligament	50	0.45
Trabecular bone	1.370	0.30
Cortical bone	13.700	0.30
Mini-screw (titanium)	110.000	0.30

A total of six finite element models were generated: three MARPE-NoDS (bone-borne) models (A–C) and three MARPE-DS (tooth-bone-borne) models (D–F) (Figure 1).

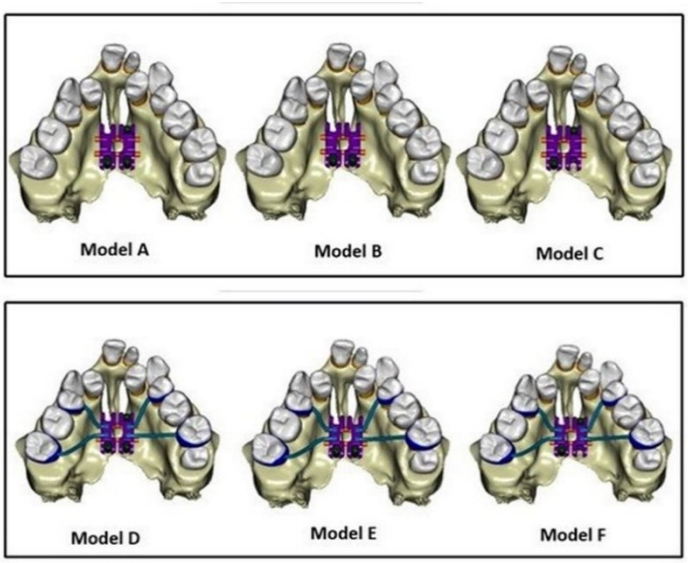

Figure 1. Finite element models evaluated: MARPE (BB) (A–C) and MARPE (TBB) (D–F).

- *MARPE-NoDS (bone-borne) model A:* A MARPE SL 9 mm (PecLab) expander was supported by three mini-screws (PecLab) (diameter: 1.8 mm; length: 10 mm; transmucosal portion: 3 mm). The mini-screws were positioned in the left and right posterior mid-palatal regions and the left anterior region.
- *MARPE-NoDS (bone-borne) model B:* A MARPE SL 9 mm (PecLab) expander was supported by two mini-screws (PecLab) (diameter: 1.8 mm; length: 10 mm; transmucosal portion: 3 mm). The mini-screws were positioned in the bilateral posterior mid-palatal regions.
- *MARPE-NoDS (bone-borne) model C:* A MARPE SL 9 mm (PecLab) expander was supported by two mini-screws (PecLab) (diameter: 1.8 mm; length: 10 mm; transmucosal portion: 3 mm). The mini-screws were positioned in the left anterior and right posterior regions.
- *MARPE-DS (tooth-bone-borne) model D:* A MARPE SL 9 mm (PecLab) expander with four-banded dental anchorage (upper second premolars and second molars) was supported by three mini-screws (PecLab) (diameter: 1.8 mm; length: 10 mm; transmucosal portion: 3 mm). The mini-screws were positioned in the bilateral posterior mid-palatal regions and the left anterior region.
- *MARPE-DS (tooth-bone-borne) model E:* A MARPE SL 9 mm (PecLab) expander with four-banded dental anchorage (upper second premolars and second molars) was supported by two mini-screws (PecLab) (diameter: 1.8 mm; length: 10 mm; transmucosal portion: 3 mm). The mini-screws were positioned in the bilateral posterior mid-palatal regions.
- *MARPE-DS (tooth-bone-borne) model F*: A MARPE SL 9 mm (PecLab) expander with four-banded dental anchorage (upper second premolars and second molars) was supported by two mini-screws (PecLab)

(diameter: 1.8 mm; length: 10 mm; transmucosal portion: 3 mm). The mini-screws were positioned in the left anterior region, anterior to the mid-palatal area, and the right posterior region.

In the MARPE-DS models, the bilateral second premolars and second molars were banded and connected using bonded interfaces with shell elements. Bonded interactions were assigned to bone-to-bone, root-to-periodontal ligament (PDL), PDL-to-bone, and tooth-to-attachment interfaces, whereas all tooth-to-tooth contacts were defined as frictionless.

Each band was connected to the expander screw base and the lingual surfaces using a 1.5 mm stainless steel wire. Each model comprised 1,286,756 elements and 5,502,525 nodes, with a processing time of 120 hours per model.

The expanders were activated transversely in 0.1 mm increments, producing a total expansion of 1.0 mm along the X-axis. Movement in the Y- and Z-axes was unrestricted to avoid constraint effects. Equivalent elastic strain (μΕ) distributions were evaluated in the maxillary palatal bone, dentoalveolar bone, and anchoring teeth. Model validation was performed using coherence analysis to confirm appropriate stress direction and distribution.

3. Results

Results are presented in occlusal views (Figure 2), lateral views (Figure 3) of the maxilla, and buccal views of the maxillary second premolars and molars (Figure 4).

In the occlusal view, all MARPE models (BB and TBB) demonstrated that strain distribution depended on both the number and, primarily, the position of the mini-implants. Strain concentrated around the mini-screws, exceeding 4000 μΕ, while also showing a more uniform distribution in adjacent regions (Figure 2).

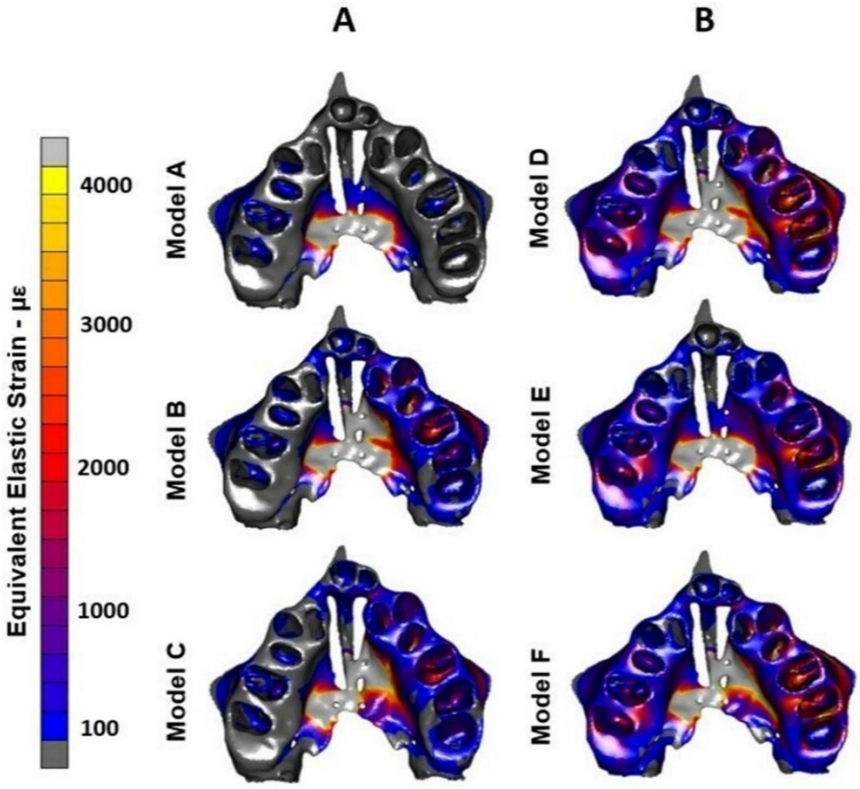

Figure 2. The strain distribution (μΕ) in the alveolar and palatal bone structures from the MARPE (BB) (A) and MARPE (TBB) (B) models under 1.0 mm of activation.

Lateral view findings were consistent with occlusal observations. Strain distribution was greater along the buccal walls and within the alveolar ridges, particularly near mini-screw sites, and varied according to their number and position. In model B, which lacked anterior palatal mini-screws, strain distribution was negligible. Strain intensity also varied with alveolar ridge size. The right ridge, reduced due to the greater cleft extent and consequently lower resistance to movement, exhibited consistently lower strain across all models (Figure 3).

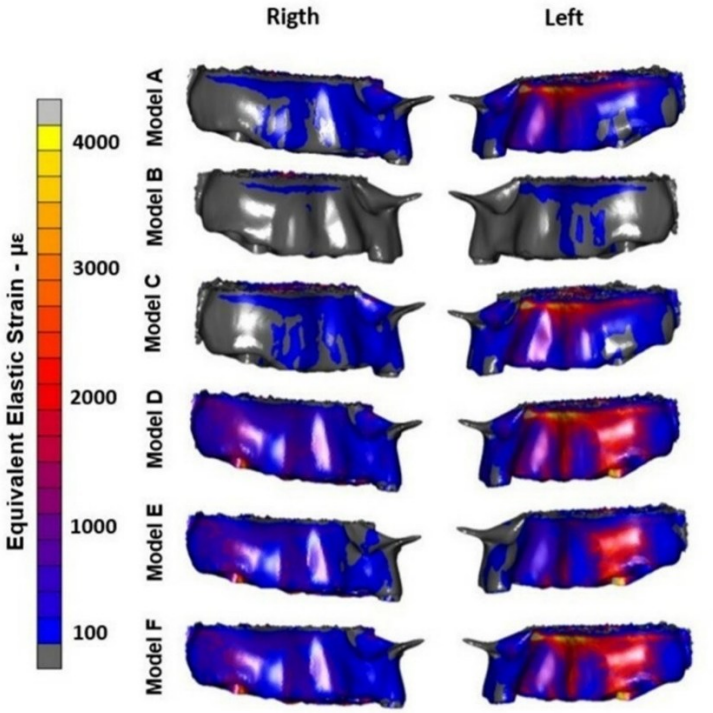

Figure 3. The right and left buccal surface views of the strain distribution (με) from the MARPE (BB) (A–C) and MARPE (TBB) (D–F) models under 1.0 mm of activation.

The presence of dental anchorage arms increased strain distribution in both occlusal and lateral views across all models. These structures generated strain even in regions without mini-screws, indicating force transmission despite the absence of direct anchorage (Figures 2 and 3).

In buccal views of the maxillary second premolars and molars, strain patterns were similar and depended on the presence of arms connecting the expander screw to the anchoring teeth. Without these arms, no strain was detected on the buccal surfaces (Figure 4). In contrast, when arms were present, all models showed significant strain exceeding 100 με at the band insertion sites, regardless of mini-screw number or distribution (Figure 4).

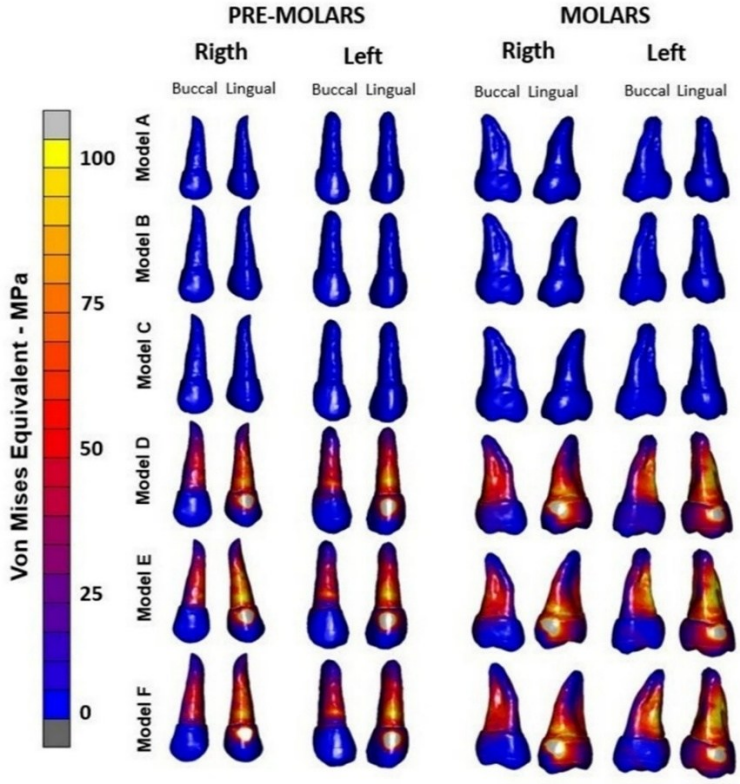

Figure 4. The strain distribution (με) on the buccal and lingual surfaces of maxillary second premolars and molars from the MARPE (BB) (A–C) and MARPE (TBB) (D–F) models under 1.0 mm of activation.

4. Discussion

This study involved a female aged 17 years with bilateral complete cleft lip and palate who had undergone secondary bone grafting at age 9, with satisfactory outcomes. The case was selected because it represents a typical presentation of this craniofacial condition, including partial palatal resorption of the graft and near-complete craniofacial growth.

Finite element analysis simulated only the initial phase of maxillary expansion using MARPE, with and without anchorage arms and varying mini-screw positioning and quantity. Activation was limited to 1.0 mm, as higher clinical values would generate excessive stress and compromise interpretability. Despite this limitation, the model demonstrated the importance of mini-screw quantity and, more critically, positioning, particularly the inclusion of at least one anterior palatal mini-screw. It also clarified the biomechanical effects of connecting arms on the dentoalveolar structures of posterior segments (Patino et al. 2024).

In occlusal views, maximum strain (>4.000 με) was concentrated around the mini-screws, supporting the requirement for a minimum diameter of 1.5 mm. Both the quantity and location of mini-screws significantly influenced strain distribution, consistent with previous reports (Mathew et al. 2016; Lee et al. 2014; Yoon et al. 2019). In lateral views, although quantity affected outcomes, configurations including at least one anterior and one posterior mini-screw (models C and F) produced deformation patterns comparable to three mini-screw models (A and D). These configurations generated greater anterior strain than models with two posterior screws only (B and E).

These findings support two considerations. First, because patients with cleft palate typically present greater anterior constriction (Yoon et al. 2019; Meng et al. 2022), placing at least one mini-screw anteriorly enhances transverse correction in this region (Mathew et al. 2016; Meng et al. 2022). Second, positioning screws within the more robust maxillary segment increases resistance and facilitates expansion aligned with anterior requirements. This asymmetrical stress distribution between cleft and non-cleft sides reflects structural differences in maxillary segments, as previously reported (Silva Filho et al. 1988; Holberg et al. 2007; Pan et al. 2007; Lee et al. 2016; Mathew et al. 2016; Lee et al. 2016) (Figure 3).

When cleft morphology limits mini-screw placement, anchorage arms may improve MARPE stability (Walter et al. 2017; Ambrosio et al. 2022). However, Moon et al. (2020) demonstrated that adding dental support increase the severity of side effects, whereas purely skeletal anchorage produces comparable skeletal outcomes with fewer dentoalveolar effects. The present findings align with this observation (Moon et al. 2020). In MARPE (BB), supported only by mini-implants, forces minimally affected lingual surfaces of posterior teeth (Figures 3 and 4).

Conversely, in (MARPE (TBB), the addition of connecting arms transmitted a substantial portion of the expansion force to all posterior alveolar ridges. The lingual contact surfaces between arms and teeth functioned as anchorage sites, generating strain values exceeding 100 με (Figures 2–4), sufficient to stimulate bone cell activity around tooth roots (Lin et al. 2015; Moon et al. 2020; Patino et al. 2024). Therefore, in patients with non-carious cervical lesions, short roots, periodontal disease, or excessive buccal inclination of posterior teeth, MARPE (BB) is preferable because it minimizes dental loading. However, when dentoalveolar integrity is compromised or sufficient mini-screw placement is not feasible, MARPE (TBB) may be indicated to enhance appliance stability during maxillary expansion in young adult patients with cleft palate.

This study has limitations. It is based on a single patient with cleft lip and palate, a condition with substantial anatomical variability. The use of a single anatomical model (N=1) was intentional to isolate mechanical variables, ensuring that observed stress and strain differences resulted solely from expander configurations, a recognized approach in biomechanical research (Walter et al. 2017; Moon et al. 2020). Additionally, only immediate mechanical effects were evaluated, without accounting for long-term biological responses or bone remodeling. The assumption of fully bonded interfaces represents an idealized condition that may overestimate strain due to the absence of load dissipation typical of non-linear interactions. Furthermore, although mesh refinement was optimized in the maxillary and dentoalveolar regions, circummaxillary sutures were excluded. Future studies incorporating the entire craniofacial complex are necessary to better characterize global skeletal responses to MARPE.

5. Conclusions

In this finite element study of young adult patients with cleft palate, mini-screw positioning had a greater influence than quantity on stress distribution in palatal and dentoalveolar structures using MARPE (BB and TBB). The inclusion of an anterior mini-screw, when feasible, is critical for inducing strain in this region. Additionally, the presence of anchorage arms significantly alters stress distribution, increasing loading on anchor teeth and posterior alveolar ridges regardless of mini-screw configuration.

Authors' Contributions: PATIÑO, A.M.B.: Conception and design; Acquisition of data; Analysis and interpretation of data; Drafting the article; Critical review of important intellectual content; Final approval of the version to be published; DOMINGOS, N.O.: Conception and design; Acquisition of data; Analysis and interpretation of data; Final approval of the version to be published; SILVA, D.T.: Conception and design; Acquisition of data; Analysis and interpretation of data; Final approval of the version to be published; KIM, K.B.: Drafting the article; Critical review of important intellectual content; Final approval of the version to be published; SOARES, C.J.: Drafting the article; Critical review of important intellectual content; Final approval of the version to be published; ALMEIDA, G.A.: Conception and design; Acquisition of data; Analysis and interpretation of data; Drafting the article; Critical review of important intellectual content; Final approval of the version to be published.

Conflicts of Interest: The authors do not have any financial interests or commercial associations to disclose.

Ethics Approval: National University of Colombia and Pediatric Hospital La Misericordia (protocol B. CIEFO-243-18).

Acknowledgments: This study was financed in part by the Coordenação de Aperfeiçoamento de Pessoal de Nível Superior - Brazil (CAPES) - Finance Code 001. We are also thankful for the support of Conselho Nacional de Desenvolvimento Científico e Tecnológico - Brazil (CNPq) and of Fundação de Amparo à Pesquisa do Estado de Minas Gerais – Brazil (FAPEMIG).

References

AMBROSIO, E.C.P., et al. Evaluation of palatal volume in children with cleft lip and palate: a comparison of two surgical protocols. *Braz Dent Sci*. 2022, **25**(3), e3299. https://doi.org/10.4322/bds.2022.e3299

CARTER, D.R., HAYE, S.W.C. Compact bone fatigue damage-I. Residual strength and stiffness. *J Biomech*. 1997, **10**(5-6), 325-37. https://doi.org/10.1016/0021-9290(77)90005-7

COBOURNE, M. T. The complex genetics of cleft lip and palate. *Eur J Orthod*. 2004, **26**(1), 7-16. https://doi.org/10.1093/ejo/26.1.7

HOLBERG, C., et al. Biomechanical analysis of maxillary expansion in CLP patients. *Angle Orthod*. 2007, **77**(2), 280–7. https://doi.org/10.2319/0003-3219(2007)077[0280:BAOMEI]2.0.CO;2

JAECQUES, S.V. et al. Individualised, micro CT-based finite element modelling as a tool for biomechanical analysis related to tissue engineering of bone. *Biomaterials*. 2004, **25**(9), 1683-96. https://doi.org/10.1016/S0142-9612(03)00516-7

KRONFELD, R.M.D. Histologic study of the influence of function on the human periodontal membrane. *J Am Dent Assoc*. 1931, 18, 1242. https://doi.org/10.14219/jada.archive.1931.0191

LAGRAVERE, M.O., et al. Transverse, vertical, and anteroposterior changes from bone-anchored maxillary expansion vs traditional rapid maxillary expansion: a randomized clinical trial. *Am J Orthod Dentofacial Orthop*. 2010, **137**(3), 304.e1-12. https://doi.org/10.1016/j.ajodo.2009.09.016

LEE, H. et al. Biomechanical effects of maxillary expansion on a patient with cleft palate: A finite element analysis. *Am J Orthod Dentofacial Orthop*. 2016, **150**(2), 313-23. https://doi.org/10.1016/j.ajodo.2015.12.029

LEE, H.K., et al. Stress distribution and displacement by different bone-borne palatal expanders with micro-implants: a three-dimensional finite-element analysis. *Eur J Orthod.* 2014, **36**(5), 531-40. https://doi.org/10.1093/ejo/cjs063

LEE, S.C., et al. Effect of bone-borne rapid maxillary expanders with and without surgical assistance on the craniofacial structures using finite element analysis. *Am J Orthod Dentofacial Orthop.* 2014, **145**(5), 638-648. https://doi.org/10.1016/j.ajodo.2013.12.029

LIN, L., et al. Tooth-borne vs bone-borne rapid maxillary expanders in late adolescence. *Angle Orthod*. 2015, **85**(2), 253-62. https://doi.org/10.2319/030514-156.1

MATHEW, A., NAGACHANDRAN, K.S. Vijayalakshmi D. Stress and displacement pattern evaluation using two different palatal expanders in unilateral cleft lip and palate: a three-dimensional finite element analysis. *Prog Orthod*. 2016, **17**(1), 38. https://doi.org/10.1186/s40510-016-0150-0

MATSUYAMA, Y., et al. Effects of palate depth, modified arm shape, and anchor screw on rapid maxillary expansion: a finite element analysis. *Eur J Orthod*. 2015, **37**(2), 188-193. https://doi.org/10.1093/ejo/cju033

MENG, W.Y., et al. The comparison of biomechanical effects of the conventional and bone-borne palatal expanders on late adolescence with unilateral cleft palate: a 3-dimensional finite element analysis. *BMC Oral Health*. 2022, **22**(1), 600. https://doi.org/10.1186/s12903-022-02640-1

MOON, H.W., et al. Molar inclination and surrounding alveolar bone change relative to the design of bone-borne maxillary expanders: A CBCT study. *Angle Orthod*. 2020, **90**(1), 13-22. https://doi.org/10.2319/050619-316.1

PAN, X., et al.. Biomechanical effects of rapid palatal expansion on the craniofacial skeleton with cleft palate: a three-dimensional finite element analysis. *Cleft Palate Craniofac J*. 2007, **44**(2), 149–54. https://doi.org/10.1597/05-161.1

PATINO, A.M.B., et al. Biomechanical behavior of three maxillary expanders in cleft lip and palate: a finite element study. *Braz Oral Res*. 2024, **38**, e010. https://doi.org/10.1590/1807-3107bor-2024.vol38.0010

PESSOA, R.S., et al. Influence of implant connection type on the biomechanical 8nvironment of immediately placed implants – CT-based nonlinear, three-dimensional finite element analysis. *Clin Implant Dent Relat Res*. 2010, **12**(3), 219-34. https://doi.org/10.1111/j.1708-8208.2009.00155.x

REES, J.S., JACOBSEN, P.H. Elastic modulus of the periodontal ligament. *Biomaterials*. 1997, **18**(14), 995-9. https://doi.org/10.1016/S0142-9612(97)00021-5

SANO, H., et al. Tensile properties of mineralized and demineralized human and bovine dentin. *J Dent Res.* 1994, **73**(6), 1205-11. https://doi.org/10.1177/00220345940730061201

SILVA-FILHO, O.G., et al. Upper dental arch morphology of adult unoperated complete bilateral cleft lip and palate. *Am J Orthod Dentofacial Orthop*. 1988, **114**(2), 154–161. https://doi.org/10.1053/od.1998.v114.a86380

WALTER, A., et al. Puigdollers A. Stability determinants of bone-borne force-transmitting components in three RME hybrid expanders – an in vitro study. *Eur J Orthod.* 2017, **39**(1), 76-84. https://doi.org/10.1093/ejo/cjw016

YANG, C.J., et al. Impact of rapid maxillary expansion in unilateral cleft lip and palate patients after secondary alveolar bone grafting: review and case report. *Oral Surg Oral Med Oral Pathol Oral Radiol*. 2012, **114**(1), 25-30. https://doi.org/10.1016/j.tripleo.2011.08.030

YOON, S., LEE, D.Y. and JUNG, S.K. Influence of changing various parameters in miniscrew-assisted rapid palatal expansion: A three-dimensional finite element analysis. *Korean J Orthod*. 2019, **49**(3), 150-160. https://doi.org/10.4041/kjod.2019.49.3.150

ZARONE, F., et al. Evaluation of the biomechanical behavior of maxillary central incisors restored by means of endocrowns compared to a natural tooth: a 3D static linear finite elements analysis. *Dent Mater*. 2006, **22**(11), 1035–44. https://doi.org/10.1016/j.dental.2005.11.034